DOI 10.1515/polyeng-2012-0128 — J Polym Eng 2013; 33(1): 33–39

Gülşen Akın Evingür and Önder Pekcan*

Drying of polyacrylamide-multiwalled carbon nanotube (MWNT) composites with various MWNTs contents: a fluorescence study

Abstract: We studied the drying of polyacrylamide (PAAm)-multiwalled carbon nanotube (MWNT) composites, prepared by free radical crosslinking copolymerization in water, with a steady state fluorescence technique. Composite gels were prepared at room temperature with pyranine (*Py*) doped as a fluorescence probe. Drying experiments were performed in air at various MWNT contents by real time monitoring of the *Py* fluorescence intensity (*I*) which increased as the drying proceeded. The Stern-Volmer equation, combined with the moving boundary diffusion model, was used to explain the behavior of *I* during drying. It was observed that the desorption coefficient (*D*) increased as the temperature increased. Drying energies (ΔE) were measured for the drying processes for each MWNT content gel, by using fluorescence, gravimetrical and volumetric methods. It is understood that ΔE values decrease by increasing MWNT content, until 1 wt% MWNT, and then increase above the level of this threshold value. The energy of drying is strongly correlated with the MWNT content in the composite. ΔE drops to its lowest value, at which conducting cluster starts to appear.

Keywords: acrylamide; drying; fluorescence; multiwalled carbon nanotube (MWNT); temperature.

***Corresponding author: Prof. Önder Pekcan,** Kadir Has University, 34083, Cibali, İstanbul, Turkey, e-mail: pekcan@khas.edu.tr
Gülşen Akın Evingür: Piri Reis University, 34940, Tuzla, İstanbul, Turkey

1 Introduction

Three-dimensional networks can be hydrophilic and/or hygroscopic and drying of these materials encompasses many fields of technology. The quantity of bound water associated with the polymer varies as per the internal structure of the gel, i.e., the monomer and cross-linking agent. Drying mechanisms in hygroscopic materials have been studied by many investigators [1, 2]. Moisture evaporates from the surface of the material to the air during the early part of drying. Once the surface water reaches the level of equilibrium content, an evaporating front forms and slowly moves into the body of the material, dividing the material into a wet region and dry region, which have different physical properties and transfer mechanisms [3]. Water diffusion and drying in polyacrylamide (PAAm) gels were investigated by Roques et al. A mathematical model with independent parameters, which analysis the critical physical phenomenon, was proposed [4]. A study based on the receding evaporating front model and on the assumption of a parabolic moisture content profile in the diffusion zone of the wet region was reported [5]. It was observed that the experimental characteristic drying curves of plaster slabs were found to depend strongly on the thicknesses of the material. An excellent review of methods for processing the data obtained from drying kinetics was written by Kemp et al. [6], where different methods for fitting and smoothing drying curves are compared. The aim is to generate curves that can be used in industrial design. Drying mechanisms of gels by diffusion [7], shear modulus [8], the status of the mechanism and the practice of drying as stresses and cracking appeared [9] were investigated [10]. A diffusive drying model, for the drying of highly shrinking materials like PAAm gel and cellulosic paste, has been reported [11]. Recently, approximate models have been used by Coumans [12] to predict the drying kinetics for slab geometry. The structural and thermodynamic properties of a water droplet enclosed in a spherical cavity, embedded in a hydrophobic material, were studied by Wallqvist et al. [13].

Recently the steady state fluorescence technique was employed for studying the drying of PAAm-NIPA composites at various temperatures [14]. The results presented in this preliminary work show that the desorption coefficient (*D*) decreased as κ-car contents were increased for a given temperature. The drying of PAAm-κ-car composite gels at various temperatures was studied by the steady-state fluorescence (SSF) technique [15, 16]. It was observed that *D* increased as the temperature was increased, for a given κ-car content.

In this work, the drying process of PAAm-MWNT composite gels, prepared with different MWNT contents, was studied by using the SSF technique at various temperatures. *Py* was used as a fluorescence probe to monitor the gel drying. It was observed that the fluorescence intensity (I) of *Py* increased as the drying time (t) was increased during the drying process. By combining the Stern-Volmer equation with the moving boundary model, values for D were determined for the drying gels prepared with various MWNT contents, at different temperatures. Drying energies (ΔE) were measured for each composite gel, and found to be first decreased and then increased at low and high MWNT content regions, respectively, by presenting minima at the conductivity threshold.

1.1 Stern-Volmer kinetics

Photophysical processes, such as fluorescence, or phosphorescence or photochemical reactions, with the concentration of a given reagent which can be a substrate or a quencher, can be explained by Stern-Volmer kinetics, which applies broadly to variations of quantum yields. In the simplest case, a plot of I versus concentration of quencher ($[Q]$) is linear, obeying the following equation [17]:

$$\frac{I_0}{I}=1+k_q\tau_0[Q] \tag{1}$$

Here, k_q is the quenching rate constant, τ_0 is the lifetime of the fluorescence probe, Q is the quencher concentration and I_0 is the I for the zero quencher content. This is referred to as the Stern-Volmer Equation.

For low quenching efficiency, ($\tau_0 k_q[Q]<<1$), Eq. (1) becomes:

$$I\approx I_0(1-\tau_0 k_q[Q]) \tag{2}$$

If one integrates Eq. (2) over the differential volume (dv) of the sample from the initial a_0 to final a_∞ thickness, then reorganization of the relation produces the following useful equation:

$$W=\left(1-\frac{I}{I_0}\right)\frac{v}{k_q\tau_0} \tag{3}$$

Here, the amount of water release (W) is calculated over the differential volume by replacing Q with W as:

$$W=\int_{a_0}^{a_\infty}[W]\,dv \tag{4}$$

Here, it is assumed that water molecules are the only quencher for the excited *Py* molecules in our system. Where v is the volume at the equilibrium drying state, which can be measured experimentally, k_q was obtained from separate measurements by using Eq. (1), where the infinity equilibrium value of water release, W, was used for each sample. The measured values of v and I at equilibrium drying conditions were used to calculate k_q for each drying experiment, separately.

1.2 Moving boundary diffusion model

The moving interface can be marked by a discontinuous change in concentration, as in the absorption by a liquid of a single component from a mixture of gases, or by a discontinuity in the gradient of concentration as in the progressive freezing of a liquid [18]. When the diffusion coefficient is discontinuous at a concentration c, i.e., the diffusion coefficient is zero below c and constant and finite above c, then the total amount (M_t) of diffusing substance desorbed from the unit area of a plane sheet of thickness a at time t is given by the following equation:

$$\frac{M_t}{M_\infty}=2\left[\frac{D}{\pi a^2}\right]^{1/2}t^{1/2} \tag{5}$$

where D is a diffusion coefficient at concentration c_1. Here $M_f=ac_1$ is the equilibrium value of M_t. If one assumes that the diffusion coefficient of polymer segments in the gel is negligible compared to the desorption coefficient, D, of water, then Eq. (5) can be written as follows:

$$\frac{W}{W_\infty}=2\left[\frac{D}{\pi a^2}\right]^{1/2}t^{1/2} \tag{6}$$

Here, it is assumed that M_t is proportional to the amount of water molecules released, W, at time, t.

2 Experimental

Commercially available MWNTs were bought from Cheap Tubes Inc., USA. They are 10–30 μm long, with an inner diameter of 5–10 nm, an outer diameter of 20–30 nm, a density of approximately 2.1 g/cm^3 and a purity >95 wt%. They were used, as supplied, in black powder form without further purification. A stock solution of MWNTs was prepared following the manufacturers regulations: nanotubes were dispersed in deionized (DI) water, with the aid of polyvinylpyrrolidone (PVP) (Merck, Germany), in proportions of

10 parts MWNTs: 1–2 parts PVP: 2000 parts DI water, by using ALEX ultrasonic equipment for 3 h at room temperature.

Composite gels were prepared by using 2 M acrylamide (AAm, Merck, Germany) with 0.1–15 wt% of MWNTs stock content at room temperature. The linear component (AAm), the initiator [ammonium persulphate (APS), Merck, Germany], the crosslinker [N,N′ methylenebisacrylamide (BIS), Merck, Germany], and the accelerator [tetramethylethylenediamine (TEMED), Merck, Germany], were dissolved in distilled water. The initiator and *Py* concentrations were kept constant at 7×10^{-3} M and 4×10^{-4} M, respectively, for all samples. The solution was stirred (200 rpm) for 15 min to achieve a homogenous solution. All samples were deoxygenated by bubbling nitrogen for 10 min just before the polymerization process [19]; each pre-composite gel solution of 5 ml was poured into a cylindrical glass tube and injector for the drying experiment. Before drying was started, composites were cut into discs with a diameter of 10 mm and a thickness of 4 mm from the injector. Disc shaped gel samples were placed on the wall of a 1 cm path length square quartz cell filled with air and water, for the drying experiment.

The *I* measurements were carried out using a Model LS-50 spectrometer (Perkin-Elmer, USA), equipped with a temperature controller. All measurements were made at the 90° position and spectral bandwidths were kept at 5 nm. Disc-shaped gel samples were placed on the wall of a 1 cm path length square quartz cell for the drying experiments. *Py* in the composite gels was excited at 340 nm during the *in situ* fluorescence experiments and emission intensities of the *Py* were monitored at 427 nm as a function of *t*. The position of the PAAm-MWNT composite gel was behind the hole in the cell and fixed by stainless steel wire and the incoming light beam for the fluorescence measurements. Here, one side of the quartz cell was covered by black cardboard, with a circular hole which was used to define the incoming light beam and limit its size to the dimensions of the gel disc [20].

At the same time, a gravimetric measurement was performed by measuring the weight. The distance and thickness of the PAAm-MWNT composite gel were also measured to calculate the volume of the PAAm-MWNT composite gel from the formula for a cylinder's volume. The initial thickness is constant for the all samples.

3 Results and discussion

Figure 1 shows the emission spectra of *Py* from the PAAm-MWNT composite gel with 3 and 10 wt% MWNT contents during drying in air at 30°C and in 150 min. It can be seen that, as the MWNT content is increased, fluorescence

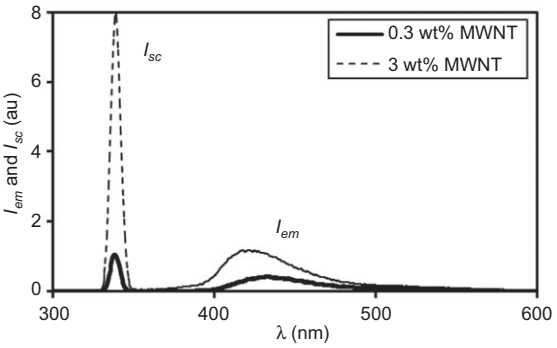

Figure 1 Emission spectra of pyranine (*Py*) from composites during drying in air, for 0.3 and 3 wt% MWNT content gels at 60°C and in 135 min.

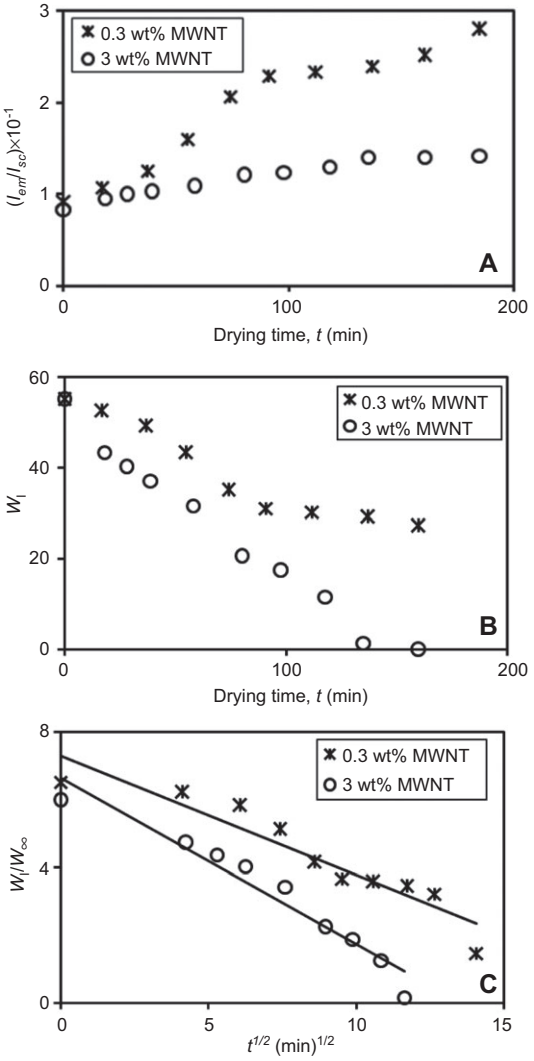

Figure 2 (A) Corrected fluorescence intensities of pyranine (*Py*), *I* (=I_{em}/I_{sc}) versus drying time (*t*), (B) the plots of the water release (*W*) versus *t* and (C) the normalized plots of *W* versus $t^{1/2}$ for polyacrylamide (PAAm)-multiwalled carbon nanotube (MWNT) composite gel dried in air measured by fluorescence technique for 0.3 and 3 wt% MWNT content samples at 60°C, respectively.

emission intensity (I_{em}) decreases relative to the scattered light intensity (I_{sc}). Since the decrease in I_{sc} corresponds to the decrease in turbidity of the drying gel, the corrected light intensity (I) was introduced as I_{em}/I_{sc} to eliminate the turbidity effect. As far as the correction of fluorescence emission is concerned, a totally empirical formula was introduced to produce the meaningful results for the fluorescence quenching mechanisms. Here, the main idea is to eliminate the structural fluctuation due to the frozen blobs and holes [21] during drying, by using I_{sc}, i.e., one has to produce the corrected I by dividing emission intensity, I_{em}, to scattering intensity, I_{sc}, to exclude the effect of turbidity of the gel on the fluorescence emission intensity and elaborate the Stern-Volmer model by using solely I.

The variations of I versus t, during drying of the composite gel at 60°C for 0.3 and 3 wt% MWNT content samples, are presented in Figure 2A. As t is increased, the quenching of the excited *Py* decreases, due to an increase in the water release from the drying PAAm-MWNT composite gel. It has also to be noted that quenching becomes more efficient at high MWNT contents, indicating that MWNTs are good quenchers for the excited *Py* molecules [22–27]. In order to quantify these results, a collisional type of quenching mechanism may be proposed for I, emitted from the gel sample during the drying process by using Eq. (3). The value of τ_0 is already known [17], so W can be calculated from the measured I values in each drying step. Figure 2B presents the W_I versus t. The normalized plots of W versus $t^{1/2}$ for 0.3 and 3 wt% MWNT content sample at 60°C are presented in Figure 2C, where the fit of the data to Eq. (6) produced the desorption coefficients, D_I, which are listed in Table 1 and plotted in Figure 3A. D_I values increased as temperature was increased for a given MWNT content, as expected.

Table 1 Experimentally measured parameters of polyacrylamide (PAAm)-multiwalled carbon nanotube (MWNT) composites for various temperature and MWNT content during the drying process.

wt% MWNTs	T (°C)	$D_I \times 10^{-9}$ (m²/s)	$D_w \times 10^{-9}$ (m²/s)	$D_v \times 10^{-9}$ (m²/s)
0	30	14.10	1.29	0.45
	40	15	1.40	0.49
	50	26	3.40	1.58
	60	48.67	4.40	1.81
0.3	30	2.46	2.83	3.05
	40	4.53	4.99	4.76
	50	8.56	9.04	8.09
	60	9.15	9.15	12.5
0.6	30	2.30	2.40	2.90
	40	3.17	3.15	2.76
	50	6.08	8.39	6.64
	60	7.37	8.72	11.5
1	30	2.29	2.04	2.60
	40	2.57	2.06	2.72
	50	4.70	3.29	3.11
	60	5.28	5.67	5.02
3	30	2.30	2.60	2.99
	40	6.23	2.76	3.29
	50	8.39	3.41	4.18
	60	10.2	6.36	6.16
5	30	2.35	2.90	3.29
	40	8.65	3.11	4.07
	50	12.1	3.86	4.51
	60	12.7	6.56	6.29
10	30	2.46	3.05	3.44
	40	9.88	4.39	4.14
	50	14.3	5.38	5.38
	60	14.2	7.47	6.52
15	30	4	3.54	4
	40	10.4	4.65	4.92
	50	16.4	6.52	6.25
	60	17.6	8.39	7.69

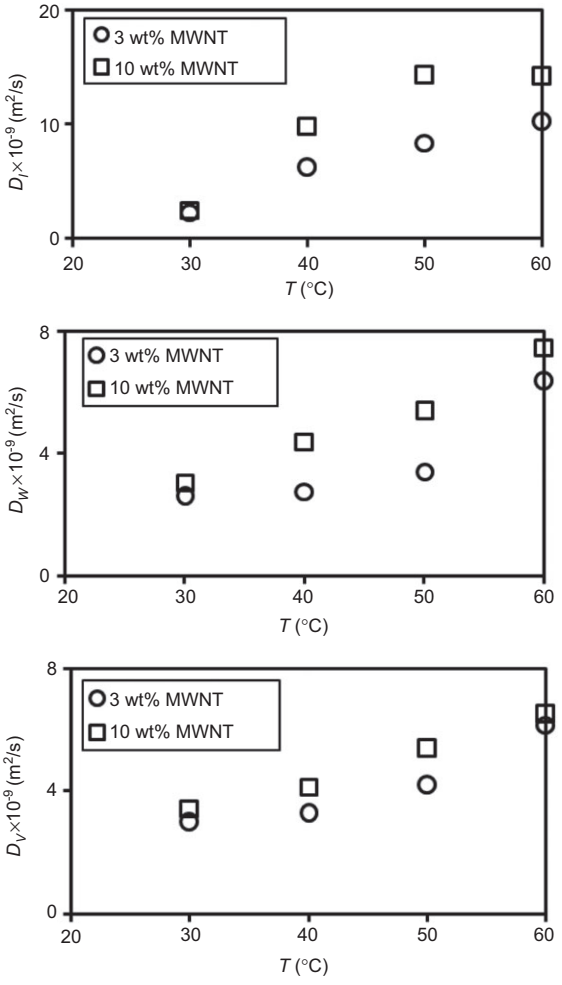

Figure 3 Desorption coefficients versus temperature measured by (A) fluorescence, (B) gravimetrically, and (C) volumetric techniques for 3 and 10 wt% MWNT content samples, respectively.

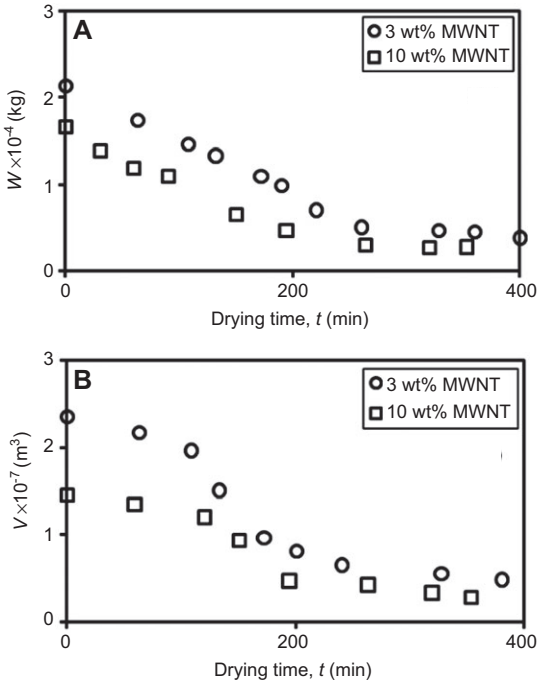

Figure 4 The plots of the water release (*W*) and *V* versus drying time (*t*), for polyacrylamide (PAAm)-multiwalled carbon nanotube (MWNT) composite gel dried in air and measured (A) gravimetrically, and (B) by the volumetric technique for 3 and 10 wt% MWNT content samples at 30°C, respectively.

Water desorption from the drying PAAm-MWNT composite gel, prepared at various MWNT content, was also studied by using the gravimetrical methods at different temperatures. The plots of *W* versus *t* are presented in Figure 4A at 30°C for 3 and 10 wt% MWNT content gels, respectively. The fits of *W* to Eq. (6) for the gels dried at 30, 40, 50 and 60°C, for various MWNT contents, produced desorption coefficients (D_W) which are listed in Table 1 and plotted in Figure 3B. A similar increase in D_W as that for D_I was observed as the temperature was increased.

The variations in volume, *V*, of PAAm-MWNT composite gels during the drying process are also monitored. The plots of the volume *V*, versus *t* for PAAm-MWNT composite gels, dried in air, are presented in Figure 4B. The data in Figure 4B are fitted to the following relation produced from Eq. (6):

$$\frac{V}{V_\infty}=2\left(\frac{D}{\pi a^2}\right)^{1/2} t_d^{\,1/2} \tag{7}$$

Here it is assumed, that the relation between *W* and *V* is linear. Then, using Eq. (7), the volumetric desorption coefficients (D_V) were determined and listed in Table 1 and plotted in Figure 3C versus temperature. Again, it is seen that D_V values increased as the temperature increased, which was similar to the D_I and D_W behavior. Here, we have to emphasize that desorption coefficients are much larger for the higher MWNT content composites, predicting that carbon nanotubes contribute to the desorption process during drying, i.e., water molecules move faster in tube channels than they do in the polymeric environment.

The behavior of the desorption coefficients (D_I, D_W, D_V) versus *T* predicts that $D - T$ relation may obey the following Arrhenius law:

$$D=D_0\, exp\,(-\Delta E/kT) \tag{8}$$

where ΔE is the energy of drying, *k* is Boltzmann's constant, and D_0 is the desorption coefficients at $T=\infty$ for each technique. The logarithmic form of Eq. (8) is presented in Figure 5 for the data obtained by fluorescence, gravimetrical and volumetric techniques, respectively,

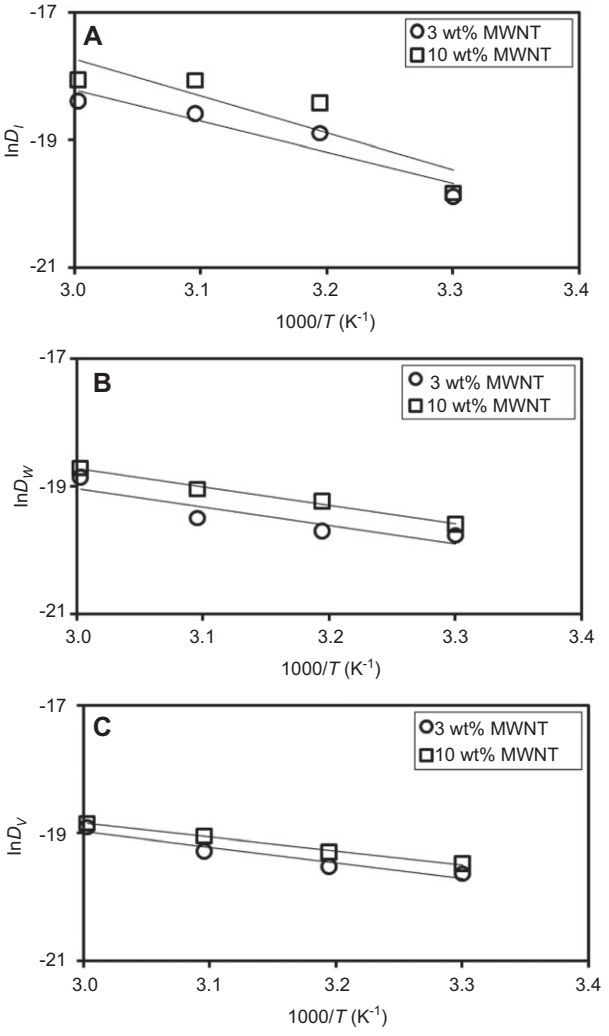

Figure 5 Linear regressions of desorption diffusion coefficients versus reverse temperature measured by (A) fluorescence, (B) gravimetrically, and (C) volumetric techniques for 3 and 10 wt% MWNT content gel samples, respectively.

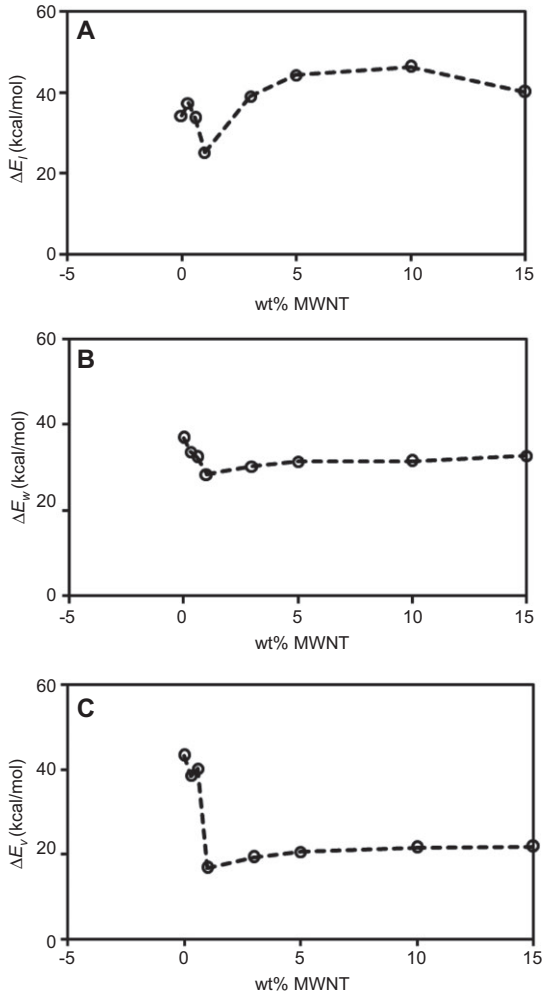

Figure 6 Energy versus wt% MWNT content measured by (A) fluorescence, (B) gravimetrically, and (C) volumetric techniques, respectively.

from which ΔE values are produced and plotted in Figure 6A, B and C, respectively. Here, we have to point out that the deviation in Figure 5A at 30°C most probably originates from the MWNT quenching of excited *Py*. In other words, at high temperatures, MWNT becomes a more effective quencher for pyranines (Merck, Germany), indicating that nanotubes are good quenchers for the fluorescence probes [22–25].

ΔE decreased until 1 wt% MWNT, and then tended to increase, as shown in Figure 6, for all measurement techniques. This is probably related to the fact that the drying behavior of composite hydrogels is obviously different from that of pure PAAm hydrogel. Here, ΔE behaved differently below and above the critical MWNT (1 wt%) content, at which the conductivity percolation cluster starts to appear [19]. Below the critical value, composite gel is more elastic and the energy needed for drying decreases as the composite system reaches 1 wt% MWNT. At this point, the energy requirement for drying is minimal, due to the formation of percolation clusters from the carbon nanotubes, which helps the water molecules to run faster and exit from the composite gel system. However, above the critical point (1 wt% MWNT), the composite gel is quite stiff, due to the formation of an infinite network, which resists the shrinking process, and as a result, the system spends a larger amount of energy on the drying process at this region.

4 Conclusion

Our experiments present a study of the drying kinetics of PAAm-MWNT composite gels with various MWNT contents. The fluorescence quenching method was employed to monitor the drying processes. A moving boundary model, combined with the Stern-Volmer kinetics, was used to measure D for drying. The experimental results indicate that D increased as the temperature increased. When MWNTs are added, the effect becomes stronger. Here, the quenching takes place basically by water molecules, which played the role during collisional quenching with *Py* molecules, i.e., as the water molecules desorb from the composite, the quenching decreases, resulting in am increase in I. The role of MWNT during the drying of composites, is to create more voids and holes, besides its static quenching background effect. In summary, high MWNT content composites dry faster above the critical value (1 wt% MWNT). It is also understood that the energy needed for drying is different below and above the critical value of MWNT, at which the conducting percolation cluster starts to appear. It is noted that the fluorescence technique is more powerful than the other classical techniques, providing information at a molecular level. As far as engineering applications are concerned, “drying” is a very important field in coating, food and pharmaceutical industries. This work introduces basic parameters for the drying processes in PAAm-MWNT composites, which can find important applications in the above mentioned fields.

Acknowledgments: Experiments were done in the Spectroscopy Laboratory in the department of Physics Engineering of Istanbul Technical University.

Received October 2, 2012; accepted October 31, 2012; previously published online January 5, 2013

References

[1] Harmathy TZ. *Ind. Eng. Chem. Fundam*. 1969, 8, 92–103.
[2] Mikhailov MD. *Int. J. Heat Mass Transfer* 1975, 18, 797–804.
[3] Hawlader MNA, Ho JC, Qing Z. *Drying Technol*. 1999, 17, 27–47.
[4] Roques MA, Zagrouba F, Sobral PD. *Drying Technol*. 1994, 12, 1245–1262.
[5] Derdour L, Desmorieux H, Andrieu J. *Drying Technol*. 2000, 18, 237–260.
[6] Kemp IC, Fyhr BC, Laurent S, Roques MA, Groenewold CE, Tsotsas E, Sereno AA, Bonazzi CB, Bimbenet JJ. *Drying Technol*. 2001, 19, 15–34.
[7] Scherer GW. *J. Non-Cryst. Solids* 1989, 107, 135–148.
[8] Scherer GW. *J. Non-Cryst. Solids* 1989, 109, 183–190.
[9] Scherer GW. *J. Non-Cryst. Solids*, 1992, 147–148, 363–374.
[10] Scherer GW, *J. Non-Cryst. Solids* 1989, 109, 171–182.
[11] Jomma W, Aregba W, Puiggali JR, Quintard M. *Drying*. 1991, 91, 110–120.
[12] Coumans WJ. *Chem. Eng. Process* 2000, 39, 53–68.
[13] Wallqvist A, Gallicchio E, Levy RM. *J. Phys. Chem. B* 2001, 105, 6745–6753.
[14] Evingur GA, Pekcan Ö. *Adv. Polym. Tech*. 2012, in press.
[15] Evingur GA, Pekcan Ö. *J. Fluoresc*. 2011, 21, 1531–1537.
[16] Pekcan Ö, Evingur GA. *e-polymers* 2011, 054, ISSN:1618–7229.
[17] Birks J. *Photopyhsics of Aromatic Molecules*, Wiley Interscience: New York, 1971.
[18] Crank J. *The Mathematics of Diffusion*, Clarendon Press: Oxford, 1975.
[19] Aktaş DK, Evingur GA, Pekcan Ö. *Compos. Interfaces* 2010, 17, 301–318.
[20] Evingur GA, Pekcan Ö. *Polym. Compos*. 2011, 32, 928–936.
[21] Kara S, Pekcan Ö. *J. Appl. Polym. Sci*. 2001, 80, 1898–1906.
[22] Qu L, Martin RB, Huang W, Fu K, Zweifel D. *J. Chem. Phys*. 2002, 117, 8089–8094.
[23] Liu L, Wang T, Li J, Guo Z-X, Dai L, Zhang D, Zhu D. *Chem. Phys. Lett*. 2003, 367, 747–752.
[24] Alvero M, Atienzar P, Bourdelande JL, Garcia H. *Chem. Phys. Lett*. 2004, 384, 119–123.
[25] Zhang Y, Yuan S, Zhou W, Xu J, Li Y. *J. Nanosci. Nanotechnol*. 2007, 7, 1–10.
[26] Pan B, Cui D, Ozkan CS, Ozkan M, Xu P, Huang T, Liu F, Chen H, Li Q, He R, Gao F. *J. Phys. Chem C* 2008, 112, 939–944.
[27] Pan B, Cui D, Xu P, Ozkan C, Feng G, Ozkan M, Huang T, Chu B, Li Q, He R, Hu G. *Nanotechnology* 2009, 20, 125101(1-9).